ANL-8105
LMFBR Safety

ARGONNE NATIONAL LABORATORY
9700 South Cass Avenue
Argonne, Illinois 60439

A PARAMETRIC STUDY OF PRESSURE GENERATION AND SODIUM-SLUG ENERGY FROM MOLTEN-FUEL-COOLANT INTERACTIONS

by

D. H. Cho, W. L. Chen,
and R. W. Wright*

Reactor Analysis and Safety Division

August 1974

*Present address: Division of Reactor Safety Research,
U. S. Atomic Energy Commission, Washington

TABLE OF CONTENTS

LIST OF FIGURES

LIST OF TABLES

NOMENCLATURE

a	$1 - \delta/R$
A	heat-transfer area per gram of heated coolant, $cm^2\ g^{-1}$
C_f	specific heat of fuel, $cal\ g^{-1}\ °K^{-1}$
C_p	specific heat of coolant at constant pressure, $cal\ g^{-1}\ °K^{-1}$
C_v	specific heat of coolant at constant volume, $cal\ g^{-1}\ °K^{-1}$
h	heat-transfer coefficient, $cal\ cm^{-2}\ sec^{-1}\ °K^{-1}$
k_f	thermal conductivity of fuel, $cal\ cm^{-1}\ sec^{-1}\ °K^{-1}$
L_f	latent heat of fusion of fuel, $cal\ g^{-1}$
P	pressure in the fuel-coolant mixing zone, atm
R	fuel-particle radius, cm
t	time, sec
t_h	characteristic heat-transfer time of fuel particle, sec
t_m	fragmentation and mixing time constant, sec
T	temperature of heated coolant, °K
T_f	average temperature of fuel, °K
T_m	melting point of fuel, °K
V	specific volume of heated coolant, $cm^3\ g^{-1}$
w	mass ratio of fuel to sodium in the mixing zone
dQ/dt	heating rate per gram of coolant, $cal\ sec^{-1}\ g^{-1}$

Greek Symbols

α_f	thermal diffusivity of fuel, $cm^2\ sec^{-1}$
δ	penetration thickness, cm
ρ_f	density of fuel, $g\ cm^{-3}$

A PARAMETRIC STUDY OF PRESSURE GENERATION AND SODIUM-SLUG ENERGY FROM MOLTEN-FUEL-COOLANT INTERACTIONS

by

D. H. Cho, W. L. Chen, and R. W. Wright

ABSTRACT

A parametric study has been performed using a rate-limited model of molten-fuel-coolant interactions previously developed. The study considered a 2-ft-long molten zone across the FFTF core, in which 1250 kg molten fuel at 3400°K were mixed with 196 kg sodium at 922°K. A few less severe cases were examined as part of the parameter variations. The effects of variations in system parameters upon pressure-time histories and sodium-slug energies were investigated. The process of sodium heating by the fuel was reformulated in order to take into account a finite rate of fragmentation and mixing.

I. INTRODUCTION

A model of molten-fuel-coolant interactions has been developed that incorporates various rate-limiting processes. The rate processes involved in the model are characterized by a number of physical parameters. At present, the magnitudes of many of these parameters are unknown or very difficult to estimate. To provide guidance for experiments and future analyses, therefore, the consequences of parameter variations need to be investigated within reasonable ranges. To this end, a parametric study of pressure-time histories and sodium-slug energies has been performed. The results are summarized in this report.

The parametric study considered a 2-ft-long molten zone across the FFTF core in which 1250 kg molten fuel at 3400°K was mixed with 196 kg sodium coolant at 922°K. A few less severe cases were also examined as part of parameter variations. The parameters varied include fuel-particle size, rate of fragmentation and mixing, molten-zone length, and initial volume of noncondensable gas present in the interaction zone. As in Ref. 1, the heat transfer was limited by the conduction resistance of the fuel alone. No account was taken of possible mechanisms of heat-transfer reduction caused by the presence of gas or sodium vaporization. In a few cases, however, the effect of a complete heat-transfer cutoff after a certain amount of heating was examined for comparison.

In Ref. 1, two different approximations were used for the heating of sodium by the molten fuel. The process of sodium heating has been reformulated in order to investigate the effect of various fragmentation and mixing rates. The reformulation is discussed in Sect. II. Section III examines parametrically the pressure-time histories for an initial period of the order of the acoustic unloading time. Sodium-slug energies are discussed in Sect. IV, considering a one-dimensional model of the sodium-slug

motion. Section V describes a simple method used to take into account the latent heat of fusion of the molten fuel.

II. EFFECT OF FRAGMENTATION AND MIXING RATES ON THE PROCESS OF SODIUM HEATING

In the preliminary calculations reported in Ref. 1, two different approximations for the process of sodium heating by the molten fuel were used. The first approximation was a quasi-steady-state heat transfer in which a constant heat-transfer coefficient was assumed. In the second approximation, transient conduction was assumed, which applies to the case of instantaneous fragmentation and mixing. As we shall see in Sect. III, the quasi-steady-state heat-transfer approximation accounts in a rough way for a finite rate of fragmentation and mixing. In this case, however, the fragmentation and mixing time is not an independent parameter. It is determined by the fuel-particle size. Thus, a new formulation is needed to consider a fragmentation and mixing time which is independent of the fuel-particle size.

We shall assume the following form for the heating rate dQ/dt of the sodium in the fuel-coolant mixing zone:

$$\frac{dQ}{dt} = hA\ (T_f - T) \quad , \tag{1}$$

with

$$hA = (hA)_o \left[\sqrt{\frac{3}{\pi}}\sqrt{\frac{t_h}{t}} + 1\right]\left[1 - \exp\left(-\frac{t}{t_m}\right)\right] \quad , \tag{2}$$

where

$$(hA)_o = \frac{C_f w}{t_h} \quad \text{and} \quad t_h = \frac{R^2}{3\alpha_f} \quad .$$

Here t_m is a characteristic measure of the rate of fragmentation and mixing, and will be called the fragmentation and mixing time constant. Note that $(hA)_o$ is the value of hA used in the quasi-steady-state heat-transfer approximation of Ref. 1 and that t_h is a characteristic heat-transfer time for each fuel particle. Equation (2) does not describe any particular mechanisms of fragmentation and mixing. Rather, it represents a convenient way of examining the effects of the fuel-particle size or the rate of fragmentation and mixing. The physical meaning of the fragmentation and mixing time constant may differ, depending upon the accident situations under consideration. However, Eq. (2) may be regarded as the product of

$$h = \frac{k_f}{\sqrt{\pi\alpha_f t}} + \frac{k_f}{R}$$

and

$$A = A_o \left[1 - \exp\left(- \frac{t}{t_m} \right) \right] ,$$

with

$$A_o = \frac{3w}{\rho_f R} ,$$

where h is the heat-transfer coefficient for each fuel particle dispersed in the sodium and A is the heat-transfer area available per gram of the heated sodium. The quantity A_o is the final value of A when the fragmentation and mixing is complete.

Equation (2) assumes that the heat transfer is limited by the fuel-conduction resistance alone. It does not take into account such a thermal resistance as might occur if the fuel particles were surrounded by a film of gas or sodium vapor.

Figure 1, in which $hA/(hA)_o$ is plotted against t/t_h, shows Eq. (2) in dimensionless form. Two broken curves indicate the approximations of

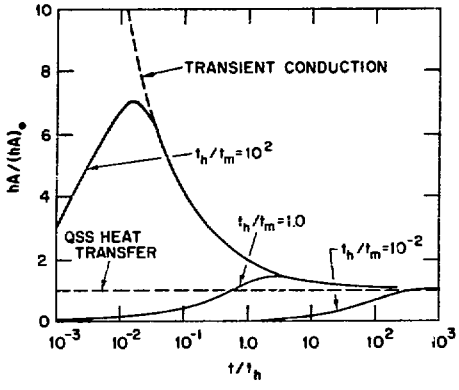

Fig. 1.
Heat Transfer with a Finite Fragmentation and Mixing Rate as given by Eq. (2). ANL Neg. No. 900-619.

transient conduction and quasi-steady-state heat transfer used in Ref. 1. The case of instantaneous fragmentation and mixing corresponds to $t_m = 0$. This case can better be described by the transient-conduction solution of Ref. 1. It will be seen in Sect. III, however, that the difference between the transient-conduction solution and Eq. (1) with $t_m = 0$ is negligibly small.

III. PRESSURE-TIME HISTORIES

The one-dimensional formulation of the acoustic constraint described in Ref. 1 is here used to examine the variation of the pressure-time histories as a result of variation of system parameters. Within the limitations of the one-dimensional formulation, the results are equally applicable both to a single-subassembly accident and to a whole-core accident. The acoustic formulation is accurate up to the unloading time when the shock wave is effectively terminated. For an FFTF subassembly, the unloading time is about 2 msec.

Eleven different cases of parameter variations were considered. Table 1 summarizes the parameters and initial conditions used, and gives the peak shock pressures calculated. The calculations were made only for an initial period of the order of the acoustic unloading time. Figures 2 to 5 show the pressure-time histories. Unless noted otherwise, the pressure pulses shown occurred during the rapid heating of the liquid sodium with boiling suppressed. Several selected histories of the sodium temperature are given in Figures 6 and 7. The latent heat of fusion of the fuel was taken into account using the simple method of equivalent temperature difference discussed in Sect. V.

We now discuss the effects of various parameters as shown in Figures 2 to 5. Case 3 will be used as the reference case.

(1) Figure 2 shows the effect of the fragmentation and mixing time for a wide range of the time constant. As the fragmentation and mixing time constant, t_m, is increased, the peak pressure is decreased, and the rise time becomes longer. In fact, there is no appreciable shock pressure for $t_m = 1$ sec (Case 4). In this case, the pressure increases slowly while the heated sodium remains a subcooled liquid. Case 1, for which $t_m = 0$, represents the case of instantaneous fragmentation and mixing. It may be considered as an approximation of the transient conduction solution given in Ref. 1.

Comparison of Case 1 with the transient conduction solution (indicated by a broken curve) shows that the difference between the two cases is small and may be neglected. Thus it appears that the form of the sodium-heating rate given by Eq. (1) is adequate for describing the heating process, including the limiting case of instantaneous fragmentation and mixing. Figure 2 also indicates that the case of quasi-steady-state heat transfer of Ref. 1 (indicated by a broken curve) corresponds roughly to a fragmentation and mixing time constant of about 3 msec. This value of the time constant applies to the fuel-particle radius of 117 μ. For a different particle size, the quasi-steady-state heat-transfer approximation would account for a different effective fragmentation and mixing time constant, and this time constant is proportional to the square of the fuel-particle radius.

(2) Figure 3 shows that the peak pressure decreases with increasing fuel-particle size. The fuel-particle radius has a similar effect upon the pressure-time histories as the fragmentation and mixing time constant. Both quantities influence the overall heating rate in a similar way. The fuel-particle radius used in Case 3 (reference case) was 117 μ, which is the median of the particle-size distribution observed in laboratory experiments. In Case 5, the particle radius was 23.4 μ, which corresponds to the 10th percentile of the distribution. In Case 6, it was 585 μ, which corresponds to the 90th percentile of the distribution.

(3) In Case 7, we considered a molten-fuel-coolant interaction which may occur following sodium reentry into a voided core. The void is assumed to be filled with a noncondensable gas at atmospheric pressure. Because of the void, the amount of liquid sodium available for the interaction is reduced. Case 7 assumes that the amount of the heated sodium is half that of the reference case (Case 3), whereas the amount of the molten fuel is

TABLE 1. Pressure-time Histories

Case		1	2	2A	3	4	5	6	7*	7A*	8	9
Initial Conditions		T(Fuel) = 3400°K;** T(Na) = 922°K; P = 1.6 atm; V(Na) = 1.26 cc/g .										
t_m, msec		0	0.1	1.0	10	1000	10	10	10	10	10	10
R, μ		117	117	117	117	117	23.4	585	117	117	117	117
L_m, ft		2	2	2	2	2	2	2	2	2	1	0.2
W		6.38	6.38	6.38	6.38	6.38	6.38	6.38	12.76	6.38	6.38	6.38
V_{go}, cc/g Na		None	None	None	None	None	None	None	1.26	0.113	None	None
Peak Pressure	P, atm	6225	4483	2246	748	---	2735	172	---	742	384	79
	t, msec	0.113	0.316	0.933	3.51	---	1.22	8.66	---	3.52	3.36	3.22

NOTE

t_m = fragmentation and mixing time constant (msec);

R = fuel particle radius (μ); L_m = molten zone length (ft);

W = fuel-sodium mass ratio; V_{go} = initial volume of noncondensable gas (cc/g Na).

* See the text.

** The fictitious initial fuel temperature is 3962°K (see Sect. V).

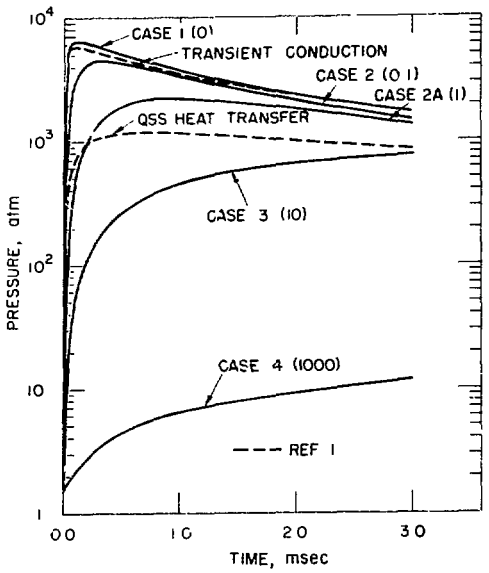

Fig. 2.
Pressure-time Histories; Effect of Fragmentation and Mixing Time. ANL Neg. No. 900-866.

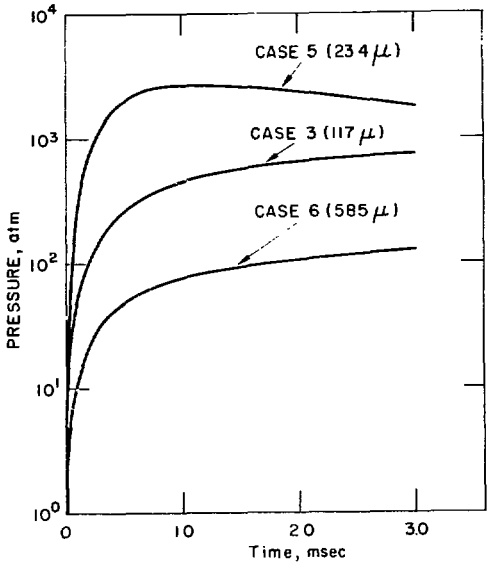

Fig. 3.
Pressure-time Histories; Effect of Fuel Particle Size. ANL Neg. No. 900-864.

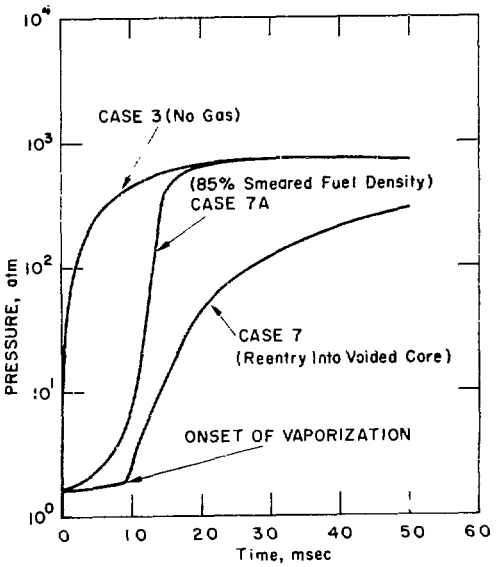

Fig. 4.
Pressure-time Histories; Effect of Gas Volume. ANL Neg. No. 900-862.

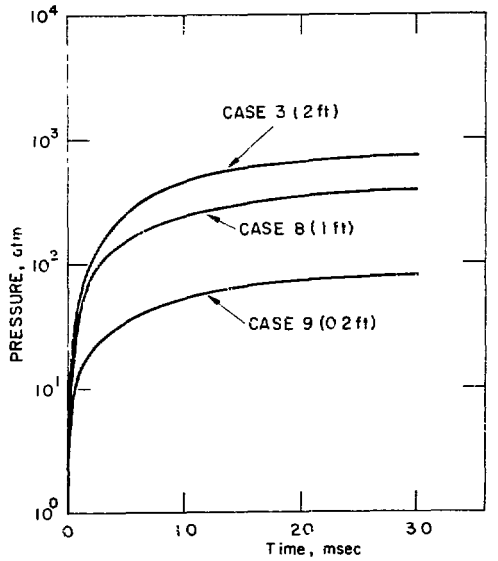

Fig. 5.
Pressure-time Histories; Effect of Molten-zone Length. ANL Neg. No. 900-865.

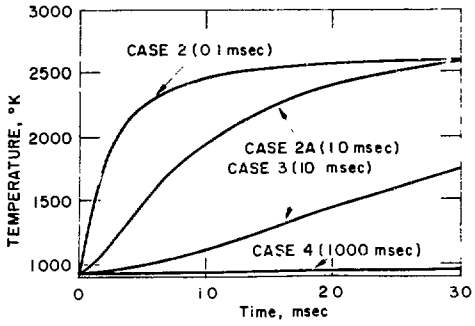

Fig. 6.
Sodium Temperature-time Histories; Effect of Fragmentation and Mixing Time. ANL Neg. No. 900-860.

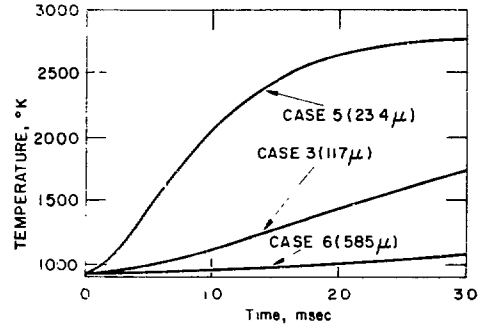

Fig. 7.
Sodium Temperature-time Histories; Effect of Fuel-particle Size. ANL Neg. No. 900-861.

unchanged. Figure 4 compares Case 7 with the reference case. In Case 7, there was no significant pressure rise during the liquid-phase heating. Most increase in pressure occurred while the heated sodium was in the two-phase region. In these calculations, it is assumed that the void does not reduce the heat transfer from the fuel into the sodium.

Case 7A examines the cushioning effect of the void volume inherent in the 85% smeared fuel density. It is assumed that the molten fuel contains the same gas volume as the original void volume inherent in smeared density of 85%. The initial gas volume in the interaction zone is then 0.113 cc/g sodium. Figure 4 shows that the initial pressure rise is somewhat delayed, but the peak pressure differs little from that of the reference case (Case 3).

(4) Figure 5 shows that the peak pressure increases almost in proportion to the molten-zone length, but its time of occurrence changes little. This effect of the molten-zone length has previously been discussed in an analytic examination of the peak pressure (Ref. 1, Appendix 3).

IV. SODIUM-SLUG ENERGIES

In the analysis of hypothetical whole-core accidents, the primary concern is with the kinetic energy of the sodium slug that impacts upon the reactor vessel head. To examine the slug energy parametrically we shall consider a 2-ft-long molten zone across the FFTF core, in which 1250 kg molten fuel initially at 3400°K is mixed with 196 kg sodium initially at 922°K. A few cases involving smaller amounts of molten fuel and sodium will be examined as part of parameter variations.

The one-dimensional formulation of inertial constraint described in Ref. 1 is used to calculate the kinetic energy of the sodium slug at the time of impact on the vessel head. This slug energy represents the work done by the expansion of the heated sodium up to the time of impact. For this parametric study, it is assumed that no structural deformation occurs, so that all the work done appears as kinetic energy of the sodium slug. The one-dimensional formulation appears to be sufficient for the present

parametric study, although it may not describe adequately details of the motion of the sodium slug above the core.

Figure 8 shows the one-dimensional model used. The zone of molten-fuel-coolant interaction expands against the inertia of a 520-cm-long sodium slug whose cross-sectional area is equal to that of the reactor vessel. We assume that the pressure in the cover-gas region remains constant at 1 atm despite the obvious compression due to the slug motion. The initial gap of the cover-gas region was taken to be 50 cm.

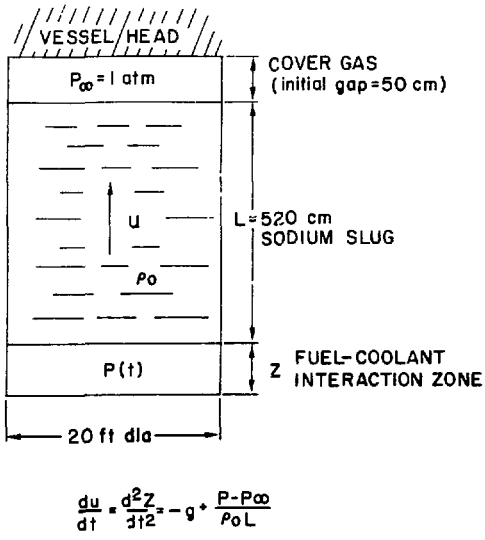

Fig. 8.
One-dimensional Model of Sodium-slug Motion. ANL Neg. No. 900-863.

Table 2 summarizes the parameters and initial conditions used for 10 different cases. Table 3 presents the results for the 10 cases in which a continuous heat transfer was assumed up to the time of impact. In the first three cases, the effect of a heat-transfer cutoff was also examined, and the results are given in Table 4. The latent heat of fusion of the fuel was taken into account using the equivalent temperature-difference method described in Sect. V.

There are some uncertainties in the results given in Tables 3 and 4, because the sodium properties used are not reliable at high temperature and pressure, especially in the region near the critical point. The absolute magnitudes of the results may thus differ, depending on the sodium properties used. However, the results indicate the following salient effects of the parameters involved.

(1) The work done up to the time of impact decreases with decreasing heating rate, whether caused by increasing the fuel-particle size or the fragmentation and mixing time constant. In Case 1, the heat transfer is assumed to be infinitely fast, which would be the case if the fragmentation and mixing were instantaneous and the fuel-particle size infinitely small. The work done in Case 1 represents the thermodynamic upper limit, such as calculated by Hicks and Menzies.[2] Note that the thermodynamic upper limit is four times greater than the work done in Case 3, in which the

TABLE 2. Calculations of Slug Energy; Initial Conditions and Parameters

Case	1	2	3	4	5	6	7*	7A*	8	9
Initial Conditions	T(Fuel) = 3400°K;** T(Na) = 922°K; V(Na) = 1.26 cc/g; P = 1.41 atm									
Total Fuel Mass, kg	1250	1250	1250	1250	1250	1250	1250	1250	625	125
Total Sodium Mass, kg	196	196	196	196	196	196	98	19[illegible]	98	19.6
t_m, msec	Infinitely Fast Heat Transfer	0.1	10	1000	10	10	10	10	10	10
R, μ		117	117	117	23.4	585	117	117	117	117
L_m, ft	2	2	2	2	2	2	2	2	1	0.2
W	6.38	6.38	6.38	6.38	6.38	6.38	12.76	6.38	6.38	6.38
V_{go}, cc/g Na	None	None	None	None	None	None	1.26	0.113	None	None
NOTE	The above cases correspond to those listed in Table 1 except Case 1. In Case 1, we assume that the heat transfer is infinitely fast, so the sodium is in thermal equilibrium with the fuel.									

* See the text (Sect. III).

** The fictitious initial fuel temperature is 3962°K (see Sect. V).

TABLE 3. Sodium-slug Energies with Continuous Heat Transfer

Case		1	2	3	4	5	6	7	7A	8	9
Final Sodium Conditions	State	all vapor	all vapor	all vapor	two-phase	all vapor	two-phase	all vapor	all vapor	all vapor	all vapor
	P, atm	---	29.9	32.7	21.9	---	27.7	28.1	32.2	19.4	5.1
	V, cc/g	75.6	75.6	75.6	75.6	75.6	75.6	151	75.6	151	756
	T, °K	2299*	2304	2329	1647	2522	1703	2978	2375	2255	2091
Final Fuel Temp, °K		2299*	2333	2370	3183**	2530	2964	3013	2415	2289	2114
Slug-impact Velocity, cm/sec		8305	4775	4085	2410	6998	2970	4305	4070	3366	1929
Time of Impact, msec		6.5	12.9	23.1	74.2	10.8	41.7	20.1	22.7	26.2	38.2
Work, J/g Na		2163	715	523	182	1536	277	1162	519	711	1167
Work, J/g UO_2		339	112	82.0	28.6	241	43.4	91.1	81.4	111	183
Total Work, MW-sec		424	140	103	35.7	301	54.2	114	102	69.6	22.9

* Because of uncertainties in the equation of state used, the calculation ignored the latent heat of sodium vaporization. The actual fuel and sodium temperatures would have been lower than those indicated.

** Actually, the fuel is at the melting point ($\sim$3100°K) with 85% solidified.

TABLE 4. Sodium-slug Energies with Heat-transfer Cutoff

Case		1X	2X	3X
Initial Conditions and Parameters		Same as Case 1 of Table 2	Same as Case 2 of Table 2	Same as Case 3 of Table 2
Assumptions for Heat-transfer Cutoff		Complete cutoff after instantaneous thermal equilibrium between the fuel and sodium	Complete cutoff occurs at unloading time of 1.98 msec (see the text)	Complete cutoff occurs at unloading time of 2.68 msec (see the text)
Final Sodium Conditions	State	two-phase	two-phase	two-phase
	P, atm	9.5	27.4	3.7
	V, cc/g	75.6	75.6	75.6
	T, °K	1475	1700	1321
Final Fuel Temp, °K		3017	2858	3661*
Slug-impact Velocity, cm/sec		4773	4506	1076
Time of Impact, msec		10.9	13.3	69.5
Work, J/g Na		714	637	36.3
Work, J/g UO_2		112	99.8	5.7
Total Work, MW-sec		140	125	7.1

*Actually, the fuel is at the melting point ($\sim$3100°K) and is all molten.

fuel-particle radius was 117 μ and the fragmentation and mixing time constant was 10 msec (reference case).

(2) Table 4 presents the results of three cases in which a heat-transfer cutoff was considered. Case 1X assumes instantaneous thermal equilibrium between the molten fuel and the sodium, followed by adiabatic expansion of the heated sodium. The work done is about a third of the thermodynamic upper limit of Case 1.

In Cases 2X and 3X, it was assumed that the heat transfer was terminated when the unloading rarefaction wave completely depressurized the heated sodium, thereby causing flashing. For an FFTF subassembly, the loading length of sodium column is about 7 ft, and the corresponding acoustic unloading time is 1.9 msec. The heat-transfer cutoff was assumed to occur 1.9 msec after the pressure in the heated sodium reached half the peak value. For Case 2X, the cutoff time was 1.9 + 0.08 = 1.98 msec, and for Case 3X, 1.9 + 0.78 = 2.68 msec.

Comparison of Cases 2 and 2X indicates that the heat-transfer cutoff reduces the work done only by 10%. However, there is an order-of-magnitude difference between Cases 3 and 3X. This is understandable if we note the difference in the fragmentation and mixing time constant between Cases 2X and 3X. In Case 2X, the fragmentation and mixing time (0.1 msec) is shorter than the heat-transfer cutoff time (1.98 msec), so that most of the sodium heating is completed before the cutoff occurs. In Case 3X, the fragmentation and mixing time (10 msec) is longer than the heat-transfer cutoff time (2.68 msec), so that only a small amount of heat is transferred before the heat transfer is terminated.

(3) As explained in Sect. III, sodium reentry into a voided molten core was considered in Case 7. The total work done (or the amount of work per gram of UO_2) in this case was 10% larger than that of the reference case (Case 3). The difference appears to reflect the effect of the fuel-to-sodium mass ratio rather than that of the gas volume. Note that this mass ratio for Case 7 (= 12.76) is closer to the optimum value* than in Case 3 (= 6.38).

The effect of the compliance of the void volume inherent in 85% smeared density fuel was examined in Case 7A. Comparison of Cases 7A and 3 suggests that the void volume in the fuel has little effect on the work.

(4) In Cases 8 and 9, the effect of the molten-zone length was examined. Other parameters were identical with those used in the reference case (Case 3). A comparison of Cases 8 and 9 with Case 3 shows that the total work done decreases with decreasing molten-zone length, but the decrease is not quite proportional to the molten-zone length. In fact, the amount of work per gram of UO_2 or sodium increases with decreasing molten-zone length. This is so because, in order for the sodium slug to impact on

---

* The optimum value refers to the fuel-to-sodium mass ratio when the work done is maximum, as observed in thermodynamic calculations. The optimum mass ratio depends on the final pressure of expansion. When the pressure is 1 atm, the optimum mass ratio is about 10. For Case 7, the final pressure is 28 atm, and the optimum mass ratio is about 13.

the head, 1 g of the heated sodium must expand to a larger volume (hence, a lower pressure) in Cases 8 and 9 than in Case 3, resulting in a large amount of work per gram of sodium or UO_2.

(5) As a matter of curiosity, the work done in Cases 1 and 1X was also calculated, assuming the heated sodium to be a perfect gas. In both cases, the work done by the expansion of the heated sodium is given by the same formula:

$$\text{Work} = \frac{P_i V_i}{n - 1}\left[1 - \left(\frac{V_i}{V_f}\right)^{n-1}\right], \tag{3}$$

where

$$n = \frac{C_p + C_f w}{C_v + C_f w} \quad \text{for Case 1}$$

and

$$n = \frac{C_p}{C_v} \quad \text{for Case 1X.}$$

Subscripts i and f denote the initial and final conditions of the expansion, respectively. With

$$C_v = \frac{3}{23}\ \text{cal/g-°C};\quad C_p = \frac{5}{23}\ \text{cal/g-°C};\ \text{and}\ C_f w = 0.765\ \text{cal/g-°C},$$

Eq. (3) gives 3665 J/g sodium for Case 1, which is 70% larger than the work given in Table 3. For Case 1X, Eq. (3) gives 1529 J/g sodium, which is about twice as much as the work given in Table 4.

(6) In the calculations, the assumption was made that all the work done by the molten-fuel-coolant interaction was expended to produce the kinetic energy of the sodium slug. In reality, however, a certain amount of the work is absorbed in the core structure, which deforms during the pressure generation. The sodium-slug energy will then be smaller than the total work done. Moreover, as indicated earlier, there are some uncertainties in the calculations because the sodium properties used are not reliable at high temperature and pressure. Therefore, the results given in Tables 3 and 4 should be used only for comparison of the effects of various parameters. It is not appropriate to apply the values of the total work (MW-sec) as given in the tables directly to a safety evaluation of the vessel-head design.

V. LATENT HEAT OF FUSION OF FUEL

When 1 g of molten UO_2 is solidified, the latent heat liberated is 67.4 cal. If this energy were all sensible heat, the corresponding increase in UO_2 temperature would be 562°C. In other words, the latent heat is equivalent to a UO_2 temperature difference of 562°C. In the calculations

discussed in Sections III and IV, the latent heat was taken into account by using a fictitious initial fuel temperature which was obtained by adding the equivalent temperature difference, 562°C, to the true initial temperature. We shall discuss below the adequacy of this simple approximation.

Consider the solidification of a semi-infinite slab of molten fuel, initially at the melting point T_m. At time t = 0, the boundary surface is suddenly brought to temperature $T_o < T_m$. The exact solution gives[3] for the heat flux at the boundary surface

$$q_{exact} = \frac{k_f}{\sqrt{\pi \alpha_f t}} \frac{T_m - T_o}{\text{erf } \lambda} , \tag{4}$$

where λ is the solution of

$$\lambda e^{\lambda^2} \text{erf } \lambda = \frac{C_f (T_m - T_o)}{L_f \sqrt{\pi}}$$

and L_f is the latent heat of fusion of the fuel.

The simple approximation discussed above gives as an approximate heat flux at the boundary surface

$$q_{approx} = \frac{k_f}{\sqrt{\pi \alpha_f t}} \left(T_m + \frac{L_f}{C_f} - T_o \right) , \tag{5}$$

where

$$L_f / C_f = 562°C \text{ for } UO_2 .$$

From Eqs. (4) and (5), we obtain

$$\frac{q_{approx}}{q_{exact}} = \text{erf } \lambda \left(1 + \frac{L_f}{C_f (T_m - T_o)} \right) , \tag{6}$$

which is plotted as a function of $(T_m - T_o)$ in Fig. 9. We see that the method of equivalent temperature difference overestimates the heat flux. However, the difference is 10% or less when $(T_m - T_o)$ is 1000°C or higher. Therefore, when the difference between the fuel and sodium temperatures is 1000°C or higher, the method of equivalent temperature difference should be a good approximation.

To test this simple method further, the transient conduction approximation of Ref. 1 was reformulated considering molten fuel particles initially at the melting point. (Note that Ref. 1 dealt only with solid fuel particles.) The integral method employed in Ref. 1 was modified to allow for the moving boundary of solidification in the molten fuel. In this case, Eq. (21) of Ref. 1 becomes

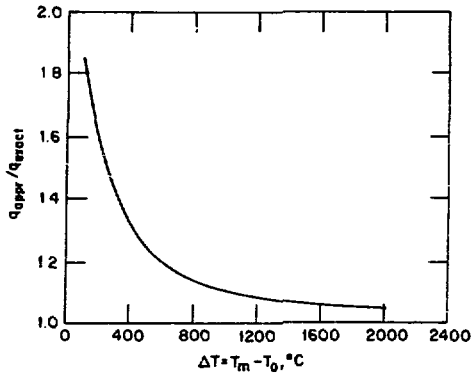

Fig. 9.
Accuracy of Equivalent Temperature-difference Method for the Latent Heat of Fusion of Fuel. ANL Neg. No. 900-620.

$$\frac{dT}{dt}\left[1 - \frac{1}{4}\left(1 + a + a^2 + a^3\right)\right] + \frac{da}{dt}\left[\frac{1}{4}\left(T_m - T\right)\left(1 + 2a + 3a^2\right) + \underline{3a^2\left(\frac{L_f}{C_f}\right)}\right] = \frac{3\alpha_f}{R^2}\,\frac{\left(T_m - T\right)}{(a - 1)}\,, \qquad (7)$$

where the underlined term represents the effect of the latent heat of fusion liberated at the moving boundary.

The reformulation was first used to calculate the pressure-time history resulting from an interaction between molten fuel initially at 3100°K (melting point of UO_2) and sodium initially at 1100°K. Other parameters were identical with those for the preliminary calculations of Ref. 1: w (fuel-to-sodium mass ratio) = 8.3, R (fuel-particle radius) = 117 μ, L_m (molten-zone length) = 35 cm, and V_{go} (noncondensable gas volume) = 0. The calculation was then made again using the method of equivalent temperature difference. In this case, the original transient conduction formulation of Ref. 1 was used with the fictitious initial fuel temperature of 3662°K (=3100°K + 562°K).

Figure 10 compares the two calculated pressure-time histories, one by the moving-boundary formulation and the other by the equivalent temperature-difference method. The latter gives a somewhat higher pressure than the former; however, the difference is quite negligible.

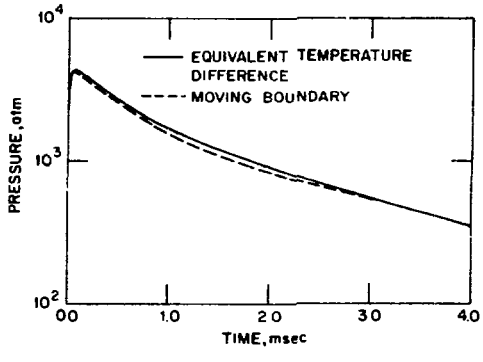

Fig. 10.
Pressure-time Histories for Transient Conduction Approximation; Comparison of Equivalent Temperature-difference Method and Moving-boundary Formulation for the Latent Heat of Fusion of Fuel. ANL Neg. No. 900-621.

From the above considerations, it seems warranted to use the simple method of equivalent temperature difference in most calculations of interest. Any inaccuracies involved are likely to give a conservative result, because the method generally overestimates the heat flux.

REFERENCES

1. D. H. Cho, R. O. Ivins, and R. W. Wright, *A Rate-limited Model of Molten Fuel-Coolant Interactions: Model Development and Preliminary Calculations*, ANL-7919 (March 1972).

2. E. P. Hicks and D. C. Menzies, *Proc. Conf. Safety, Fuels, and Core Design in Large Fast Power Reactors*, ANL-7120, p. 654 (1965).

3. H. S. Carslaw and J. C. Jaeger, *Conduction of Heat in Solids*, Second Edition, Oxford University Press, pp. 285-286 (1959).